31st Annual International Conference of the IEEE EMBS
Minneapolis, Minnesota, USA, September 2-6, 2009

Computational Hemodynamic Modeling based on Transesophageal Echocardiographic Imaging

C. Sprouse, D. Yuh, T. Abraham, and P. Burlina

Abstract—**We address the problem of hemodynamic computational modeling in the left heart complex. The novelty of our approach lies in the exploitation of prior patient specific data resulting from image analysis of Transesophageal Echocardiographic Imagery (TEE). Kinematic and anatomical information in the form of left heart chambers and valve boundaries is recovered through a level-set-based user-in-the-loop segmentation on 2D TEE. The resulting boundaries in the TEE sequence are then interpolated to prescribe the motion displacements in a computational fluid dynamics (CFD) model implemented using Finite Element Modeling (FEM) applied on Arbitrary Lagrangian-Eulerian (ALE) meshes. Experimental results are presented.**

I. Introduction

As stated by Yoganathan [1], heart and valve biodynamics and the mechanisms ensuring their proper functioning are controlled by many complex multiscale factors including the surrounding hemodynamic environment. This paper addresses the problem of computing the blood motion flow field through the left heart chambers. We believe that our computational approach will be beneficial for aiding the assessment of the heart dynamical and functional behavior. Such information can be exploited in surgical planning systems to help predict the outcome of complex reconstructive surgeries such as cardiac valvuloplasty. This work can also be used to augment TEE rendering, and assist cardiologists and clinicians in better assessing pathologies such as heart valve regurgitation, by providing a higher resolution and more complete (i.e., full vectorial) picture of the flow when compared to the current Doppler echocardiography. TEE is the imaging modality chosen for this work since it is flexible and non-ionizing and can be exploited both pre- or intra-operatively.

Mathematical modeling of cardiac physiology and biodynamics was pioneered by Peskin [2, 3], who introduced a method based on Fluid-Structure Interaction (FSI), termed the "immersed boundary" (IB) approach [4]. Ongoing work is being pursued to extend IB and address some of its reported limitations including (1) the valve's infinitely thin structural approximation, with no slip, where the fluid is ideally viscous and cannot admit discontinuities, and (2) the inability to model static loading, bending and shear behavior [5]. Yoganathan [1, 6] reported other FSI models extending IB to solve for 3D incompressible Navier-Stokes equations applied to left-ventricle motion. Reul [7] used FSI to model a single leaflet in a tube. Watton [5] extended IB to simulate a polyurethane replacement valve placed in a cylindrical tube, subject to physiologic periodic fluid flow. Einstein [8] reported a coupled FSI mitral model immersed in a domain of Newtonian blood. This model had anterior and posterior leaflets but did not include other structures such as the left ventricle. Espino's recent 2D model [9] simulated the left ventricle-generated blood flow by adding a non-anatomical inlet at the left ventricular apex.

Most prior work in heart computational modeling does not include patient specific data, with some recent exceptions [10, 11]. Howe's [11] work uses a simpler computational model inspired by computer graphics to characterize the closed mitral valve position using mass-spring dynamics, but does not address hemodynamics effects. Recent nascent "integrative" approaches to heart modeling include projects such as the cardiome [12], REO [13-16] and the Virtual Physiological Human programs [17].

The novelty of our approach compared to prior work, lies in the fact that it incorporates patient-specific anatomical and dynamical information by using 2D TEE segmentation for hemodynamics modeling. Sections II and III describe the techniques for segmentation and CFD, while Section IV reports experimental results.

II. Heart Wall Segmentation

In our proposed image-driven CFD approach, structural boundary information is obtained by first segmenting the atrial and ventricular endocardial surfaces on 2D TEE imaging data. Statistical segmentation methods characterizing intensity or texture such as [18] may be inadequate for echocardiography, because texture and intensity are not uniform in this modality. Among recent image segmentation methods, level sets (LS) [19] are of particular interest as they can be made to rely on edge rather than intensity information.

Segmentation using level sets is obtained by considering the contour of a 3D function [20]. This 3D function represents a volume which expands under a driving force $\boldsymbol{F}$. The method locates the domain boundary $C(s^*)$ by solving the evolution equation (Eq. (2)) for the stationary

C. Sprouse is with the Johns Hopkins University (JHU) Applied Physics Lab (APL). D. Yuh is with the JHU Medical School, Division of Cardiac Surgery. T. Abraham is with the JHU Medical School, Division of Cardiology. P. Burlina is with the JHU APL and the JHU Computer Science Department (e-mails: chad.sprouse@jhuapl.edu, dyuh@jhmi.edu, philippe.burlina@jhuapl.edu). We wish to thank Drs. D. DeMenthon, D. Herzka, and E. McVeigh for useful discussions on the approach.

point s^* of:

$$C(s) = \{(x,y) \mid \phi(x,y,s) = 0\}. \quad (1)$$

The evolution equation for ϕ is given by:

$$\frac{\partial \phi}{\partial t} + F \mid \nabla \phi \mid = 0 \quad (2)$$

This is called the level set equation [20, 21]. Key design choices guiding the success of the level set method are the choice of F and the selection of the stopping criteria. In our approach, the force is designed so that the curve expands or contracts to encompass a structural entity such as the intraventricular cavity.

When ϕ is updated over time using the original LS algorithm, it tends to slowly depart from the actual signed distance function, and must be periodically reinitialized, leading to inefficiencies. We follow the recent variational approach introduced by Li [22] to resolve this issue. Li includes a penalty term to evolve ϕ so that it is close to the signed distance function. Using the signed distance property $\mid \nabla \phi \mid = 1$, a new constraint can be introduced:

$$P(\phi) = \int_\Omega \frac{1}{2}\left(\mid \nabla \phi \mid -1\right)^2 dxdy \quad (3)$$

where $\Omega \subset \mathbb{R}^2$ represents the domain of ϕ. Using this metric, a new evolution equation is then expressed as:

$$\frac{\partial \phi}{\partial t} = -\frac{\delta \varepsilon}{\delta \phi} \quad (4)$$

$$\varepsilon(\phi) = \mu P(\phi) + \varepsilon_m(\phi) \quad (5)$$

where $\mu > 0$ is a weighting term that controls how closely ϕ must follow the signed distance function, and $\varepsilon_m(\phi)$ is the function that drives the curves evolution to the desired goals. $\varepsilon_m(\phi)$ is defined as:

$$\varepsilon_m(\phi) = \lambda L_g(\phi) + \upsilon A_g(\phi) \quad (6)$$

where $\lambda > 0$ and υ are weights controlling the curve length and areas penalties. The length and area terms are given by:

$$L_g(\phi) = \int_\Omega g\delta(\phi)\left|\nabla \phi\right| dxdy \quad (7)$$

$$A_g(\phi) = \int_\Omega gH(-\phi)dxdy \quad (8)$$

where $\delta(\phi)$ is the Dirac delta function and $H(\phi)$ is the Heaviside function. g is the force field derived from the TEE image driving the curve evolution. The new formulation is then summarized as:

$$\frac{\partial \phi}{\partial t} = \mu\left[\Delta\phi - \mathrm{div}\left(\frac{\nabla\phi}{\mid \nabla\phi \mid}\right)\right] + \lambda\delta(\phi)\,\mathrm{div}\left(g\frac{\nabla\phi}{\mid \nabla\phi \mid}\right) + \upsilon g\delta(\phi) \quad (9)$$

As indicated earlier our force is based on image edges:

$$g(x,y) = 1 - \left(\frac{\mid \nabla I(x,y) \mid}{M}\right) \quad (10)$$

This function behaves like an 'inverse' image map of the edges where the edge values are small (close to zero). ∇I is the intensity gradient and M its maximal value.

We have used this methodology to automatically segment myocardial wall boundaries on 2D TEE images (see experiment section). Several characteristics of ultrasonic imaging make segmentation difficult when compared to CT or MRI including decreased spatial resolution, clutter noise, and imaging artifacts (e.g., obscuration, out of plane anatomical structures emerging in 2D TEE). To address these issues, and to strike a balance between speed and accuracy, we have combined an automated method for preliminary segmentation with a user-in-the-loop inspection and correction step to yield the final segmentation fed to our CFD. Another issue with level sets is the *seeding* (initialization). Currently this is done manually and one possibility is to exploit the segmentation found for an image at time *t* to define a new seed for the frame at time *t+1*.

III. Computational Fluid Dynamics Modeling

We have developed a finite element model of the left ventricle assuming incompressible fluid properties for the blood. In contrast with methods requiring *dual-domain* models including both solid and fluid domains, with fluid-structure interaction, our model is a simpler fluid-only model. A dual model would necessitate prescribed forces while our single fluid domain model requires only prescribed endocardial wall motion, which can be directly measured using patient imagery, as explained in the previous section.

Given the prescribed wall anatomy and boundary conditions, we solve for the blood motion field. The flow velocity field v is found as the solution of the incompressible Navier-Stokes equations expressed as:

$$f = \rho\frac{\partial v}{\partial t} + \rho v \cdot \nabla v + \nabla p - \nabla \cdot \mathbf{T} \quad (11)$$

where f is the external force, $\mathbf{T}$ the stress tensor, ρ denotes the fluid density affecting the convective terms, and p is the pressure. Additionally, the dissipative term $\nabla \cdot \mathbf{T}$ is further specified as:

$$\nabla \cdot \mathbf{T} = \eta(\nabla v + \nabla v^T) \quad (12)$$

where η is the dynamic viscosity. Finally the incompressible fluid constraint is expressed as:

$$\nabla \cdot v = 0. \quad (13)$$

Pressure release boundaries were placed in the pulmonary vein and aorta to form a closed system. The boundary conditions and above equations are solved using an Arbitrary Lagrangian-Eulerian (ALE) mesh.

The final segmented boundary is represented by a time-series of rational B-splines each with an equal number of control points. Motion of the control points is specified through cubic spline interpolation from frame to frame. Motion of each boundary segment $\partial\Omega_i$ is obtained through the B-spline parameterization.

$$\partial\Omega_i = \frac{(1-s)^2 P_i + \sqrt{2}s(1-s)P_{i+1} + s^2 P_{i+2}}{(1-s)^2 + \sqrt{2}s(1-s) + s^2}, s \in [0,1] \quad (14)$$

A time-dependent domain is defined by the motion of the boundary which is discretized by the ALE mesh. The time-dependent blood flow is solved on this domain with a moving-wall boundary condition which ensures that the flow velocity is equal to the domain velocity at the boundary.

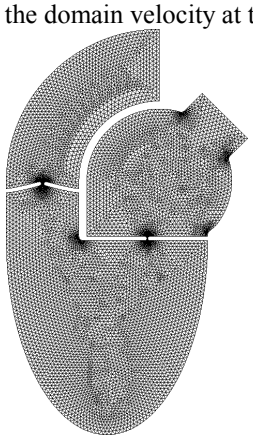

Figure 1 A simulated model for the left heart complex along with the Arbitrary Lagrangian-Eulerian mesh.

IV. RESULTS AND DISCUSSION

A preliminary experiment used a finite element model of the left heart undergoing simulated prescribed motion. We used a rudimentary anatomy for the left atrium, left ventricle, a portion of the ascending aorta, and the aortic and mitral valves. The left atrium was modeled as a circle, the aorta was a wide bent tube, and the ventricle was the bottom half of an ellipse. The model's dimensions were chosen based on clinical ultrasound imaging studies.

Left ventricular myocardial contractility was simulated by synthetically varying the intracavitary diameter of the ventricle sinusoidally with physiologic amplitudes. For the mechanical characteristics of the blood, we used typical values for the blood density and viscosity found in the literature [9] with $\rho = 1.06 \times 10^3$ kg/m^3 and $\eta = 2.7 \times 10^{-3}$ Pa$\cdot$s. The geometry and the resulting initial resting ALE mesh are shown in Figure 1. Figure 2 and Figure 3 show the resulting blood flow velocity field computed during diastolic motion (valveless example) and systolic motion (example with valves). The generated blood flow in general and specifically the presence of vortices in the atrium during diastole are consistent with physiological observations.

A second experiment involved TEE-driven modeling. Results of the application of the automated segmentation are shown in Figure 4. We have found, as in other studies [19, 23], that the LS method provided promising results. However, in our experience, it is not always immune to errors especially due the poor resolution of 2D TEE data. Another issue with LS is that of traversing anatomical boundaries which is related to the selection of stopping criteria. One last issue lies in the potentially limited field of view of ultrasound imagery which sometimes omits important anatomical features (e.g., left ventricle apex, papillary muscles, etc.). For all these reasons we felt it important to complement our approach with user intervention. Results of automated and subsequent user-based segmentation are shown in Figure 4.

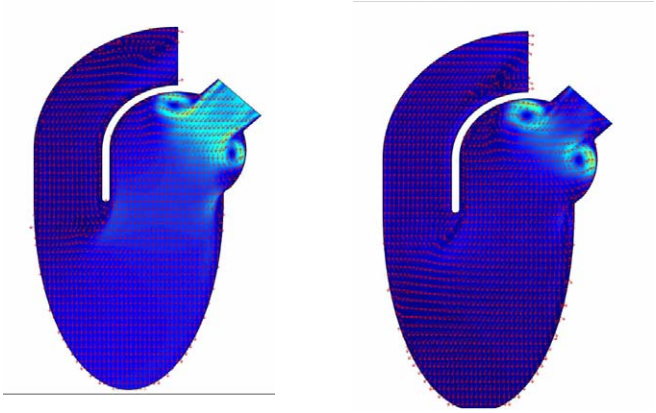

Figure 2 Result motion flow estimation obtained using a valveless model during diastole.

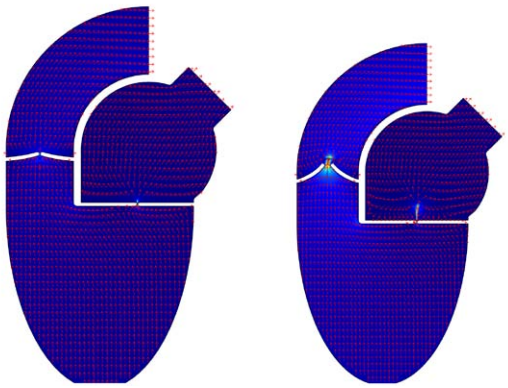

Figure 3 Flow computed in a simulated model with valves during systole.

The results of the computation of flow magnitude and direction on patient imagery are shown in Figure 5. Figure 6 shows a close up on the patient flow around the mitral valve during systole. The patient suffered from valve insufficiency and our method displays a regurgitating flow past the mitral valve leaflets which is consistent with the patient pathology. One of the limitations we have found in our method is in its handling of very large deformations such as closure of the mitral valve during early isovolumetric contraction. Such large-scale deformations cause the ALE mesh to greatly deform and the domain must be periodically remeshed. Even with remeshing, some mesh elements can become inverted at which point the solution breaks down. We intend to address these issues and other limitations cited earlier in future work.

V. CONCLUSION

We proposed a novel patient specific, TEE image driven CFD method for recovering flow in the left heart chambers. Preliminary results are presented and show the promise of the approach. Future goals are to address certain limitations

of the method to remedy ALE mesh behavior and to extend the method to 3D.

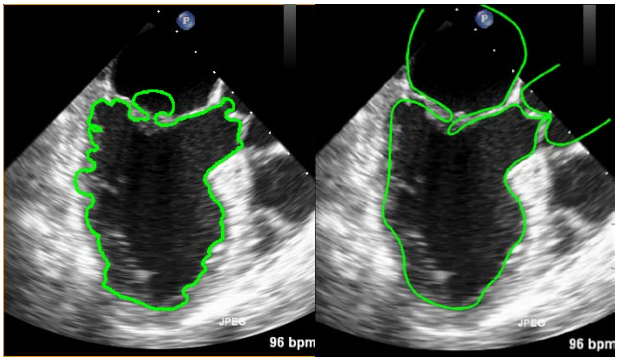

Figure 4 Result of segmentation obtained using our level set method (left) and the subsequent user-refined segmentation (right).

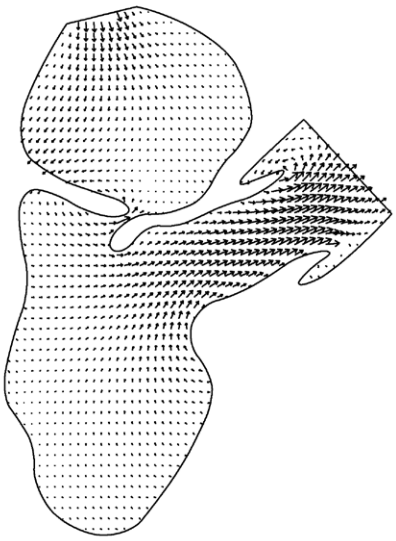

Figure 5 Result of flow computation on a model driven by TEE segmentation data.

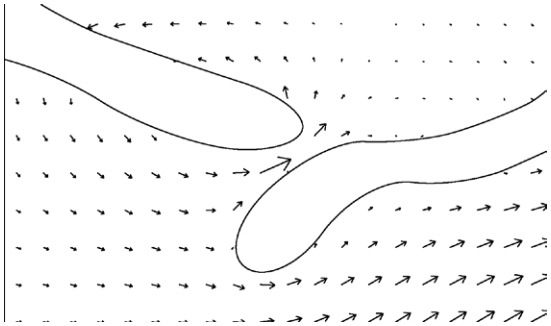

Figure 6 Detail of the computation on a model driven by TEE segmentation data showing blood regurgitating through mitral valve.

REFERENCES

[1] M. S. Sacks and A. P. Yoganathan, "Heart valve function: a biomechanical perspective," *Philos Trans R Soc Lond B Biol Sci,* vol. 362, pp. 1369-1391, 2007.

[2] C. S. Peskin, "Flow patterns around heart valves. a digital computer method for solving the equations of motion," in *Albert EinsteinCollege of Medicine*. vol. Ph.D., 1972.

[3] C. S. Peskin, *Mathematical aspects of heart physiology*: Courant Institute of Mathematical Sciences, 1975.

[4] C. S. Peskin and D. M. McQueen, "A 3D computational method of blood flow in the heart: 1. immersed elastic fibers in a viscous incompressible fluid," *Journal Computational Physics,* vol. 81, pp. 372-405, 1989.

[5] P. N. Watton, X. Y. Luo, R. Singleton, X. Wang, G. M. Bernacca, P. Molloy, and D. J. Wheatley, "Dynamic modeling of prostetic chorded mitral valves using the immersed boundary method," in *IEEE Conf. Engineering in Medicine and Biology Society,*, 2004.

[6] C. C. Vesier, J. J. D. Lemmon, R. A. Levine, and A. P. Yoganathan, "A three-dimensional computational model of a thin-walled left ventricle," in *Proceedings of the 1992 ACM/IEEE conference on Supercomputing* 1992.

[7] R. v. Loon, P. D. Anderson, and F.N. van de Vosse, "A fluid-structure interaction method with solid-rigid contact for heart valve dynamics " *Jounal of Computational Physics,* vol. 217, pp. 806-823, 2006.

[8] D. Einstein, K. Kunzelman, P. Reinhall, M. Nicosia, and R. Cochran, "Non-linear fluid-coupled computational model of the mitral valve," *J Heart Valve Dis,* vol. 14, pp. 376-385, 2005.

[9] D. Espino, M. A. Watkins, D. E. T. Shepherd, D. W. L. Hukins, and K. G. Buchan, "Simulation of blood flow through the Mitral Valve of the heart: a fluid structure interaction model," in *Proc. COMSOL Users Conference*, 2006.

[10] Z. Hu, D. Metaxas, and L. Axel, "Computational modeling and simulation of heart ventricular mechanics with tagged MRI " in *ACM symposium on Solid and physical modeling* 2005.

[11] Peter Hammer, P. d. Nido, and R. Howe, "Image based mass spring model of mitral valve closure for surgical planning," in *SPIE Medical*, 2008.

[12] J. B. Bassingthwaighte, "Design and strategy for the Cardionome project.," in *Adv. Exp. Med. Biology*, 1997.

[13] H. Delinghette, "Integrated cardiac modeling and visualization," in *Int. Conf. Medical Image Computing and Computer-Assisted Intervention*, 2008.

[14] INRIA-REO, "The INRIA REO group," 2008.

[15] N. D. D. Santos, J.-F. Gerbeau, and J. F. Bourgat, "A partitioned fluid-structure algorithm for elastic thin valves with contact," *Comp. Meth. Appl. Mech. Eng,* vol. 197, 2008.

[16] M. Astorino, J.-F. Gerbeau, O. Pantz, and K.-F. Traoré, "Fluid-structure interaction and multi-body contact. Application to the aortic valves," INRIA RR 6583 2008.

[17] EU, "The virtual physiological human EU project," 2008.

[18] A. Banerjee, P. Burlina, and F. Alajaji, "Image Segmentation and Labeling using the Polya Urn Model", IEEE Transactions on Image Processing," *IEEE Trans. Image Processing,* vol. 8, pp. 1243-1253, 1999.

[19] A. Tsai, A. Yezzi, W. Wells, C. Tempany, D. Tucker, A. Fan, W. E. Grimson, and A. Willsky, " A shape-based approach to the segmentation of medical imagery using level sets," *IEEE Trans. Medical Imaging,* vol. 22, pp. 137-154, 2003.

[20] R. Juang, P. Burlina, and A. Banerjee, "Level Set Segmentation of Hyperspectral Images Using Joint Spectral Edge and Signature Information," in *International Conference on Information Fusion*, 2008.

[21] S. Osher, "A level set formulation for the solution of the Dirichlet Problem for Hamilton-Jacobi equations," *SIAM J Math Anal,* vol. 24, pp. 1145-1152, 1993.

[22] C. Li, C. Xu, C. Gui, and M. Fox., "Level Set Evolution without Re-Initialization: A New Variational Formulation," 2005, pp. 430--436.

[23] C. Corsi, G. Saracino, A. Sarti, and C. Lamberti, "Left ventricular volume estimation for real-time three-dimensional echocardiography," *IEEE Trans. Medical Imaging,* vol. 21, 2002.